technologies

MDPI

Article

Drilling of Copper Using a Dual-Pulse Femtosecond Laser

Chung-Wei Cheng [1,*] and Jinn-Kuen Chen [2]

[1] Department of Mechanical Engineering, National Chiao Tung University, No. 1001, Ta Hsueh Road, Hsinchu 30010, Taiwan

[2] Department of Mechanical and Aerospace Engineering, University of Missouri, Columbia, MO 65211, USA; chenjnk@missouri.edu

* Correspondence: weicheng@nctu.edu.tw; Tel.: +886-3-571-2121 (ext. 55126)

Academic Editors: Chia-Lung Kuo, Jin-Chen Hsu, Chao-Ching Ho and Yuan-Jen Chang
Received: 23 December 2015; Accepted: 19 February 2016; Published: 23 February 2016

Abstract: The drilling of copper using a dual-pulse femtosecond laser with wavelength of 800 nm, pulse duration of 120 fs and a variable pulse separation time (0.1–150 ps) is investigated theoretically. A one-dimensional two-temperature model with temperature-dependent material properties is considered, including dynamic optical properties and the thermal-physical properties. Rapid phase change and phase explosion models are incorporated to simulate the material ablation process. Numerical results show that under the same total laser fluence of 4 J/cm^2, a dual-pulse femtosecond laser with a pulse separation time of 30–150 ps can increase the ablation depth, compared to the single pulse. The optimum pulse separation time is 85 ps. It is also demonstrated that a dual pulse with a suitable pulse separation time for different laser fluences can enhance the ablation rate by about 1.6 times.

Keywords: femtosecond laser; dual pulse; two-temperature model

1. Introduction

Ultrashort (pico- or femto-second) lasers have been successfully demonstrated in drilling, cutting, surface structural modification and internal modification of transparent material because of their minimal heat-affected zone [1] and high peak power intensity [2]. Many theoretical and experimental works on ultrashort laser-material interactions have been reported. In the theoretical studies on femtosecond laser ablation of metal, most works have focused on two-temperature model (TTM) [1,3–5] or hydrodynamic model [6]. Experiments with single- or multi-shot ablation or the drilling of metal under different laser parameters have also been presented, e.g., laser fluence [7–9] and pulse duration [10–12]. For example, the ablation rate of iron can be optimized by variation of the single pulse duration in the range of 0.3–3.6 ps [12]. In our previous study, both numerical simulation and experiments was performed to investigate the femtosecond laser ablation of copper by a single-shot or multi-pulses [13,14].

Recently, numerous experiments on the enhancement of metal drilling using a dual-pulse nanosecond laser have been presented [15–17]. Nanosecond laser pulses separated by several tens of nanoseconds are shown that they can enhance the material removal rates while minimizing the heat-affected zone [16]. Experiments on the ultrashort dual-pulse laser drilling of copper using different wavelengths (800 nm and 532 nm) have also been investigated [18–20]. For a pulse separation time longer than 10 ps, the resulting plasma was found to shield the target surface and consequently decrease the ablation rate. On the other hand, the enhanced grooving of the steel when using a dual-pulse

femtosecond laser was reported recently [21]. However, the optimum pulse delay time for ablation enhancement remains unclear, especially for the pulse separation time in the order of picoseconds.

In this study, the thermal ablation of copper by means of a dual-pulse femtosecond laser is investigated using a computational model, including a TTM with dynamic optical properties, two phase change models for melting and evaporation, and a phase explosion criterion for ejection of the mixture of metastable liquid droplets and vapor. The numerical results of the thermal response and the ablation depth generated by the dual-pulse femtosecond laser under different separation times and laser fluences are presented and discussed herein.

2. Modeling

In Figure 1, a copper foil is normally irradiated by a dual-pulse femtosecond laser on the front surface and the laser beam is propagated along the z-axis. The dual pulse is Gaussian in time with a full width at half maximum of t_p. The pulse separation time is t_{sep}. For simplicity without losing accuracy, the problem is approximated to be one dimensional since laser spot sizes are much larger than the thermally affected depth. The 1D TTM for electron and lattice temperature in a copper foil is expressed as follows [22,23]:

$$C_e \frac{\partial T_e}{\partial t} = \frac{\partial}{\partial z}(k_e \frac{\partial T_e}{\partial z}) - G(T_e - T_l) + S(z,t) \quad (1)$$

$$C_l \frac{\partial T_l}{\partial t} = \frac{\partial}{\partial z}(k_l \frac{\partial T_l}{\partial z}) + G(T_e - T_l) \quad (2)$$

where t is the time, T the temperature, C the heat capacity, k the thermal conductivity, G the electron-phonon coupling factor, and $S(z, t)$ the laser heat density. The subscripts e and l denote the electron and lattice, respectively. The k_l is usually neglected for pure metals due to the fact that it is two orders smaller than k_e. However, the heat conduction in the lattice should be considered in this model for which it includes solid-liquid and liquid-vapor phase change.

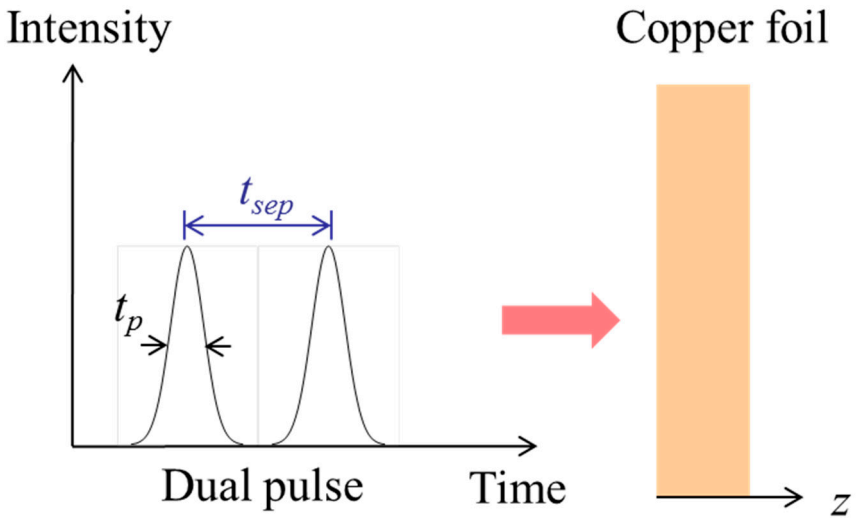

Figure 1. Dual-pulse femtosecond laser irradiated on copper surface.

The laser heat density S for a dual pulse can be expressed in a general form as [13]:

$$S(z,t) = \sum_{i=1}^{2} 0.94 \frac{[1 - R(0,t)]F_i}{t_p} \frac{1}{\delta(z,t) + \delta_b} \exp\left[-\int_0^z \frac{1}{\delta(z,t) + \delta_b} dz - 2.77 \left(\frac{t - (i-1)t_{sep}}{t_p} \right)^2 \right] \quad (3)$$

where $R(0,t)$ is the temperature-dependent surface reflectivity of the material at $z = 0$; F_i is the laser fluence of the i-pulse; $\delta(z, t) = 1/\alpha(z,t)$ is the temperature-dependent optical penetration depth; and $\alpha(z,t)$ is the absorption coefficient. The electron ballistic range δ_b added to the $\delta(z,t)$ here is to take into account the effects of the hot electron diffusion that spreads the absorbed laser energy into a deeper part of electrons. In this work, a constant value of $\delta_b = 15$ nm for copper is used [5].

In previous studies [3], constant surface reflectivity and absorption coefficient are often assumed for laser energy deposition. However, the dynamic optical properties during laser irradiation can significantly alter the irradiated laser energy absorption and influence the distribution of laser heat density, respectively. In this study, a critical point model with three Lorentzian terms is used to calculate the optical reflectivity and the absorption coefficient of copper [24].

The thermophysical properties, *i.e.*, C, k and G, control the thermal transport and temperature distributions in the laser-irradiated material. In this study, polynomial functions are used to describe the C_e and G for the copper material over a range of electron temperatures [14,25]. At a non-equilibrium condition, the k_e used is a function of electron and lattice temperature as [24]:

$$k_e = \chi \frac{(\varphi_e^2 + 0.16)^{5/4}(\varphi_e^2 + 0.44)\varphi_e}{(\varphi_e^2 + 0.092)^{1/2}(\varphi_e^2 + \xi\varphi_l)} \quad (4)$$

where $\phi_e = T_e/T_F$ and $\phi_l = T_l/T_F$. T_F is Fermi temperature; χ and ξ are constants. For copper, $T_F = 8.16 \times 10^4$ K, $\chi = 377$ W/(m·K), and $\xi = 0.139$. The bulk thermal conductivity, specific heat and mass density of copper in solid and liquid phases can be also found in [24].

If the laser fluence of a femtosecond laser pulse is sufficiently high, a solid medium can be melted and ablated through vaporization, and even by phase explosion. To accurately simulate the material removal process, the above 1D TTM is integrated with two phase change models for ultrafast melting/resolidification and evaporation, and a phase explosion model for ejection of metastable liquid and vapor. In the phase change model, the liquid-vapor interfacial velocity can be calculated from the vaporization wave model and shock wave theory [26,27]. The details of these models can be found in reference [28]. They are not described here for brevity.

For metals heated by femtosecond laser pulses, the molten material can be superheated without boiling, because the heating time is too short for the necessary heterogeneous nuclei to form. As the temperature of the superheated liquid approaches the thermodynamic equilibrium critical temperature, T_c, the tensile strength of the liquid rapidly falls to zero. Consequently, homogeneous bubble nucleation occurs at an extremely high rate. The superheated liquid thus relaxes explosively into a mixture of vapor and equilibrium liquid droplets and immediately ejected from the bulk material.

In numerical analyses of ultrafast laser ablation, it is often assumed that phase explosion takes place when the superheated liquid temperature reaches to 90% of T_c [29]. When a volume of the superheated liquid temperature reaches $0.9T_{tc}$, that material is removed under the assumption of phase explosion. The vertical size of the corresponding volume is defined as the ablation depth.

In the numerical simulation, a copper foil with an initial temperature of 300 K is irradiated on the front surface by a dual-pulse femtosecond laser with wavelength of 800 nm, pulse duration of 120 fs and a variable pulse separation time (0.1–150 ps). For each laser pulse, the lasering starts from $t = -2t_p$ and ends at $t = 2t_p$. The laser energy outside this time period is ignored, because it is too small to significantly alter the results. A number of 2500 finite volumes per μm are employed. The thermodynamic equilibrium critical temperature, T_c, is 7696 K for copper [30]. The details of the numerical iteration algorithms for modeling melting/resolidification and vaporization can be found in [31].

3. Results and Discussion

Figure 2 shows the time dependence of the calculated optical reflectivity, electron temperature and lattice temperature on the copper surface for the different laser pulses with the same total laser

fluence of 4.0 J/cm^2, *i.e.*, a single pulse with 4.0 J/cm^2 and a dual pulse of 2.0 J/cm^2 per pulse. The pulse separation times of the two dual-pulses, t_{sep}, are 10 ps and 100 ps, respectively. As shown in Figure 2a, the reflectivity decreases quickly during the laser pulse irradiation; the reflectivity at room temperature (t = −0.24 ps) is 0.962, and the minimum values for the three cases are 0.244 (t = 0.12 ps), 0.274 (t = 10.1 ps) and 0.31 (t = 100.1 ps). The time-resolved reflectivity for copper irradiated by a femtosecond laser (806 nm, 100 fs) was also presented previously [32]. The temporal reflectivity decreased from a maximum of 0.85 to a minimum of 0.23, which is similar to our single-pulse case.

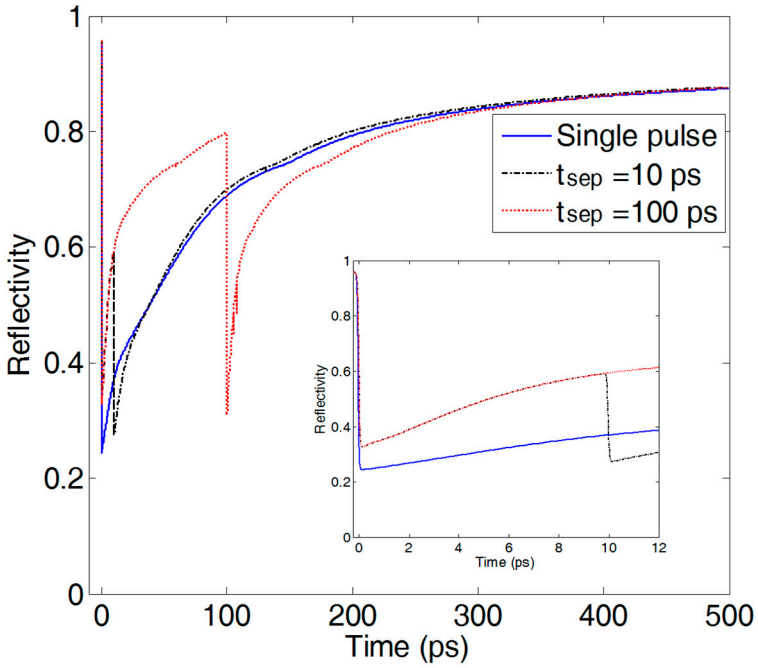

(**a**)

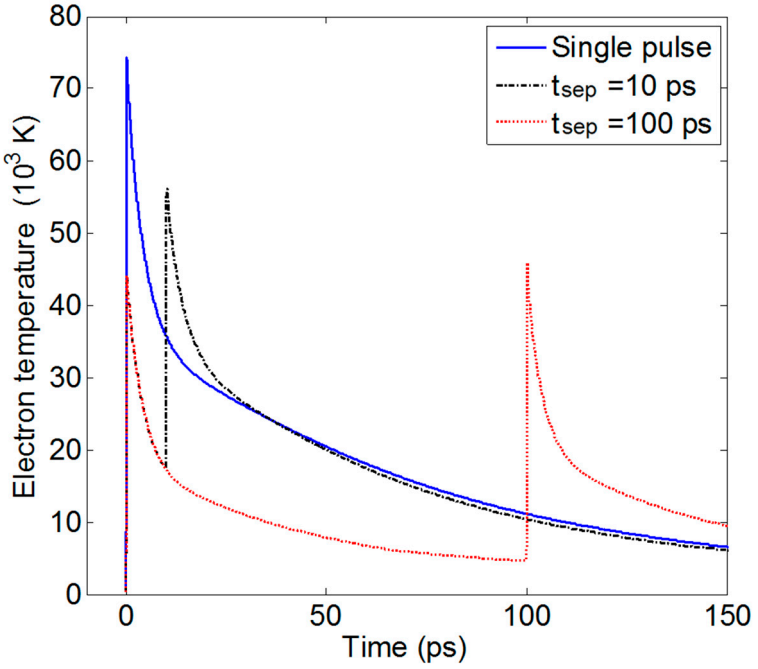

(**b**)

Figure 2. *Cont.*

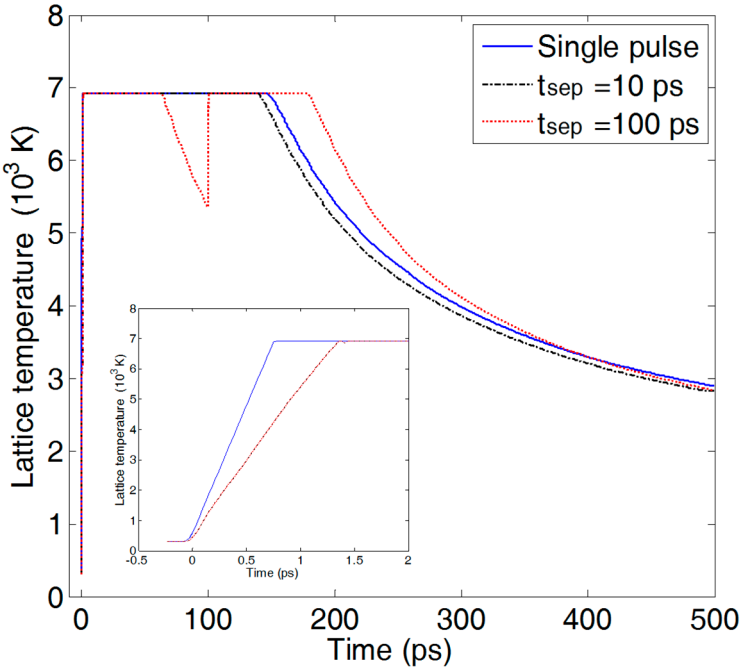

(**c**)

Figure 2. Time dependence of calculated (**a**) optical reflectivity; (**b**) electron temperature and (**c**) lattice temperature on the copper surface for different laser pulses with the same total laser fluence of 4.0 J/cm^2.

For the dual-pulse cases, the minimum reflectivity after the second pulse irradiation is usually lower than that of the first pulse. For example, in the case of t_{sep} = 10 ps (see inset), the minimum reflectivity for the first and second pulses are 0.327 and 0.274, respectively, since the high electron temperatures (see Figure 2b) excited on the copper surface after the first pulse help decrease the reflectivity for the second pulse. It was evident that these dynamic properties could alter the thermal response.

Figure 2b shows that the highest electron temperature decreases with increases in separation time; the maximum values for the three cases are 74,229 K (t = 0.12 ps), 56,029 K (t = 10.1 ps) and 45,967 K (t = 100.1 ps), respectively. In the dual-pulse cases, however, the peak electron temperature induced by the second pulse irradiation is usually higher than that by the first pulse. For example, in the case of t_{sep} = 100 ps, the peak electron temperatures induced by the first and second pulses are 44,121 K and 45,967 K, respectively. It is worth noting that the surface reflectivity before the second pulse irradiation is lower than that at room temperature (Figure 2a) due to temperature rise in material. The further decrease of the reflectivity by the second pulse increases the amount of laser energy deposited from the second pulse, and thus the electron temperature is increased to a higher level than that by the first pulse.

As shown in Figure 2c, over the timescale of a few picoseconds (see inset), the lattice is heated up via the electron-phonon collisions, and the maximum lattice temperatures after the first pulse for the three cases remain at around 6,926 K, *i.e.*, 90% of the thermodynamic equilibrium critical temperature, T_c (7696 K), which is attributed to the phase explosion. This temperature lasts for about 147 ps for the single pulse and 140 ps for the dual pulse with the pulse separation time 10 ps. However, for the dual-pulse cases with the pulse separation of 100 ps, the lattice temperature starts to drop to below 0.9 T_c at about 63 ps, and quickly reaches 0.9 T_c after the second pulse irradiation. Those time periods of temperature 0.9 T_c shown in Figure 2c indicate the occurrence of phase explosion.

The time histories of material ablation depth resulting from different laser pulses with the same total laser fluence of 4.0 J/cm^2 are shown in Figure 3a. For each case, there are two different ablation

rates. The steep ablation rate results mainly from the phase explosion, while the flatter one in from evaporation. For the dual pulse with the separation time of 100 ps, phase explosion stops at 63 ps, followed by a vaportaion, and then re-starts when the second pulse impinges onto the material. This means that a dual pulse with a separation time shorter than 63 ps, phase explosion would continue to a time instant sooner or later than the time (178 ps here) found for the single pulse. It can be found from Figure 3a that the total ablation depths by the dual-pulse with $t_{sep} \leqslant 10$ ps are smaller than that of the single-pulse case. When $t_{sep} \geqslant 30$ ps, the total ablation depth is enhanced, as compared to the single pulse. The enhancement of material ablation by a dual pulse with a longer separation time can be explained as follows. Before the second laser pulse is irradiated, there is more time for the thermal energy to be conducted into the deeper part of material. The spread of energy heats more material to or near to the state of phase explosion, leading to more material ablation by the second pulse. It can be found from Figure 3a that for the case of t_{sep} = 100 ps, the ablation depth resulting from the first and second pulses are 52 nm and 79 nm, respectively.

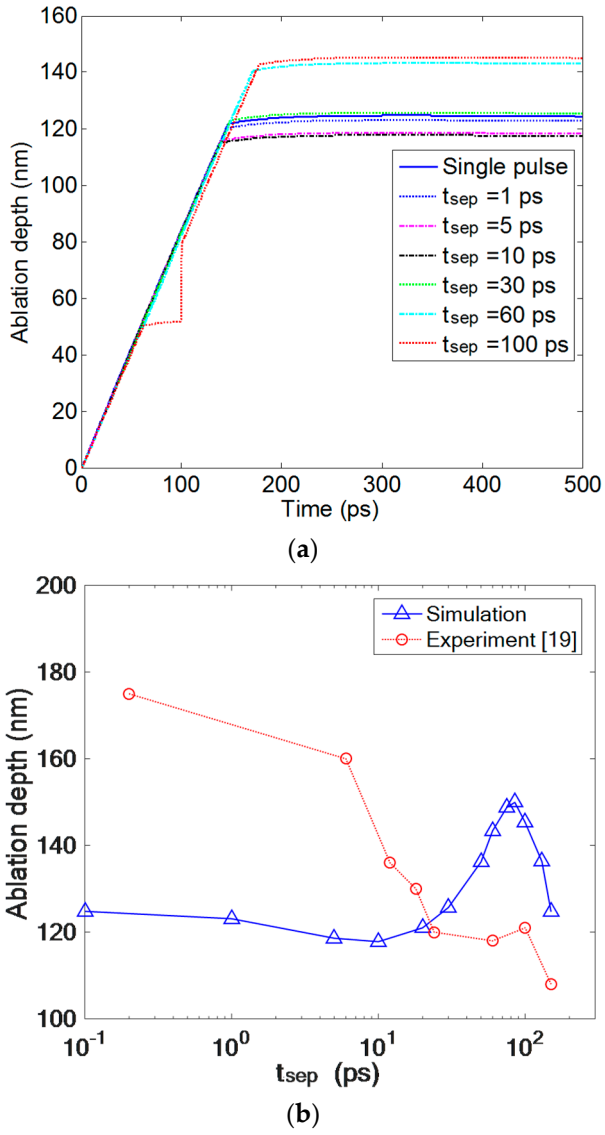

Figure 3. (**a**) Time history of ablation depth resulting from different laser pulses and (**b**) ablation depth as a function of separation time, with a total laser fluence of 4.0 J/cm^2.

The proposed method was used to predict ablation depths, as well as to compare the experimental result by [19] of two delayed femtosecond laser pulses (laser wavelength 800 nm, pulse duration 100 fs). Figure 3b shows the comparison between the simulated and experimental ablation depths with the same total laser fluence of 4.0 J/cm^2. The simulation results from Figure 3b demonstrate that an optimum value of the pulse separation time, t_{sep}, for enhancing the ablation efficiency exists. For the cases studied here with a total fluence 4.0 J/cm^2. The maximum ablation depth is about 150 nm for the dual pulse with the separation time 85 ps. It is noted, however, that the ablation depth by a dual pulse with t_{sep} < 30 ps is smaller than that by the single pulse of 125 nm.

However, the simulation ablation depths are not agreed well with those by experimental result. The simulation result for the dual pulse with t_{sep} < 10 ps is similar to the experimental results by [18,19]; e.g., the ablation depth is similar to that by the single pulse for t_{sep} < 1 ps and smaller for 1ps < t_{sep} < 10 ps. However, for t_{sep} > 10 ps, the experimental result show that the ablation depth decreases with t_{sep} in the range of 10–150 ps. The reason is that when t_{sep} > 10 ps, the plasma starts to shield the target surface and the second laser pulse is spent reheating the plasma, with no additional ablation depth resulting from the second pulse observed.

Interestingly, the study in which a dual-pulse femtosecond laser train was used to groove steel showed that the ablation depth is dramatically increased with an increase in t_{sep}, with a maximum ablation depth in the range of 5–30 ps obtained [21]. Recently, a dual-pulse femtosecond laser for ablation of silver foil in vacuum was presented [33]. It was also found that the ablation depth does not always decrease as the t_{sep} increases longer than 10 ps. For example, with a laser fluence of 106 J/cm^2, the ablation depth decreases for t_{sep} < 10 ps but increases to its maximum value for t_{sep} ~ 60 ps.

In the femtosecond laser material ablation process, it is desirable that the maximum ablation depth be obtained and that the temperature rise could be as low as possible to reduce the heat-affected zone and thermal stresses. Figure 4 shows the variation in the total ablation depth between the single and dual pulse for a total laser fluence of 3–8 J/cm^2. The ablation depth by the dual pulses with a suitable t_{sep}, *i.e.*, t_{sep} = 80, 85, 120, 145, 170 and 190 ps, is higher than that by the single pulse. The straight lines curve-fitted from the calculated data confirm the logarithmic dependence between the ablation depth and the laser fluence. The slope of the fitted line for the dual pulse is found to be higher by about 1.64 times, as compared to that for the single pulse. It is shown that the dual femtosecond pulses with suitable pulse separation time have a potential to increase material removal rates and thereby reducing the undesired thermal effects.

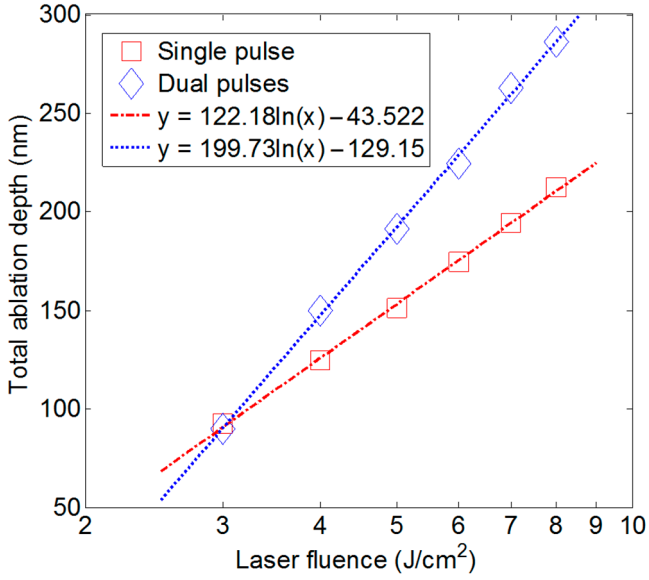

Figure 4. Variation in the ablation depth between single and dual pulses with laser fluence.

4. Conclusions

This paper reports the numerical results of thermal ablation of copper foil by a single- and dual-pulse femtosecond laser for laser fluences of 3–8 J/cm^2. It is found that a dual pulse with a total laser fluence of 4 J/cm^2 and a pulse separation time around 85 ps can increase the amount of material ablated, as compared to a single pulse. It is also demonstrated that a dual pulse with a suitable pulse separation time for different laser fluences can enhance the ablation rate by about 1.6 times. The results show that a dual-pulse femtosecond laser has a potential to improve laser drilling efficiency.

Acknowledgments: The authors would like to thank the Ministry of Science and Technology MOST 103-2218-E-009-025-MY2 for support of this research.

Author Contributions: Chung-Wei Cheng designed and implemented the simulation model, and prepared the manuscript. Jinn-Kuen Chen edited the manuscript, conceptualized the research. All authors have read and approved the final manuscript.

Conflicts of Interest: The authors declare no conflict of interest.

References

1. Nolte, S.; Momma, C.; Jacobs, H.; Tunnermann, A.; Chichkov, B.N.; Wellegehausen, B.; Welling, H. Ablation of metals by ultrashort laser pulses. *J. Opt. Soc. Am. B* **1997**, *14*, 2716–2722. [CrossRef]
2. Gattass, R.R.; Mazur, E. Femtosecond laser micromachining in transparent materials. *Nat. Photonics* **2008**, *2*, 219–225. [CrossRef]
3. Yang, J.; Zhao, Y.; Zhu, X. Theoretical studies of ultrafast ablation of metal targets dominated by phase explosion. *Appl. Phys. A* **2007**, *89*, 571–578. [CrossRef]
4. Wu, B.; Shin, Y.C. A simple model for high fluence ultra-short pulsed laser metal ablation. *Appl. Surf. Sci.* **2007**, *253*, 4079–4084. [CrossRef]
5. Byskov-Nielsen, J.; Savolainen, J.-M.; Christensen, M.S.; Balling, P. Ultra-short pulse laser ablation of copper, silver and tungsten: Experimental data and two-temperature model simulations. *Appl. Phys. A* **2011**, *103*, 447–453. [CrossRef]
6. Colombier, J.P.; Combis, P.; Bonneau, F.; le Harzic, R.; Audouard, E. Hydrodynamic simulations of metal ablation by femtosecond laser irradiation. *Phys. Rev. B* **2005**, *71*, 165406. [CrossRef]
7. Byskov-Nielsen, J.; Savolainen, J.M.; Christensen, M.S.; Balling, P. Ultra-short pulse laser ablation of metals: Threshold fluence, incubation coefficient and ablation rates. *Appl. Phys. A* **2010**, *101*, 97–101. [CrossRef]
8. Hashida, M.; Semerok, A.F.; Gobert, O.; Petite, G.; Izawa, Y.; Wagner, J.F. Ablation threshold dependence on pulse duration for copper. *Appl. Surf. Sci.* **2002**, *197*, 862–867. [CrossRef]
9. Kirkwood, S.E.; van Popta, A.C.; Tsui, Y.Y.; Fedosejevs, R. Single and multiple shot near-infrared femtosecond laser pulse ablation thresholds of copper. *Appl. Phys. A* **2005**, *81*, 729–735. [CrossRef]
10. Le Harzic, R.; Breitling, D.; Weikert, M.; Sommer, S.; Fohl, C.; Valette, S.; Donnet, C.; Audouard, E.; Dausinger, F. Pulse width and energy influence on laser micromachining of metals in a range of 100 fs to 5 ps. *Appl. Surf. Sci.* **2005**, *249*, 322–331. [CrossRef]
11. Weck, A.; Crawford, T.H.R.; Wilkinson, D.S.; Haugen, H.K.; Preston, J.S. Laser drilling of high aspect ratio holes in copper with femtosecond, picosecond and nanosecond pulses. *Appl. Phys. A* **2008**, *90*, 537–543. [CrossRef]
12. Artyukov, I.A.; Zayarniy, D.A.; Ionin, A.A.; Kudryashov, S.I.; Makarov, S.V.; Saltuganov, P.N. Relaxation phenomena in electronic and lattice subsystems on iron surface during its ablation by ultrashort laser pulses. *JETP Lett.* **2014**, *99*, 51–55. [CrossRef]
13. Wang, S.Y.; Ren, Y.; Cheng, C.W.; Chen, J.K.; Tzou, D.Y. Micromachining of copper by femtosecond laser pulses. *Appl. Surf. Sci.* **2013**, *265*, 302–308. [CrossRef]
14. Cheng, C.W.; Wang, S.Y.; Chang, K.P.; Chen, J.K. Femtosecond laser ablation of copper at high laser fluence: Modeling and experimental comparison. *Appl. Surf. Sci.* **2016**, *361*, 41–48. [CrossRef]
15. Lehane, C.; Kwok, H.S. Enhanced drilling using a dual-pulse Nd:YAG laser. *Appl. Phys. A* **2001**, *73*, 45–48. [CrossRef]

16. Forsman, A.C.; Banks, P.S.; Perry, M.D.; Campbell, E.M.; Dodell, A.L.; Armas, M.S. Double-pulse machining as a technique for the enhancement of material removal rates in laser machining of metals. *J. Appl. Phys.* **2005**, *98*, 033302. [CrossRef]
17. Wang, X.D.; Michalowski, A.; Walter, D.; Sommer, S.; Kraus, M.; Liu, J.S.; Dausinger, F. Laser drilling of stainless steel with nanosecond double-pulse. *Opt. Laser Technol.* **2009**, *41*, 148–153. [CrossRef]
18. Semerok, A.; Dutouquet, C. Ultrashort double pulse laser ablation of metals. *Thin Solid Films* **2004**, *453*, 501–505. [CrossRef]
19. Noël, S.; Hermann, J. Reducing nanoparticles in metal ablation plumes produced by two delayed short laser pulses. *Appl. Phys. Lett.* **2009**, *94*, 053120. [CrossRef]
20. Amoruso, S.; Bruzzese, R.; Wang, X.; O'Connell, G.; Lunney, J.G. Multidiagnostic analysis of ultrafast laser ablation of metals with pulse pair irradiation. *J. Appl. Phys.* **2010**, *108*, 113302. [CrossRef]
21. Liebig, C.; Srisungsitthisunti, P.; Weiner, A.M.; Xu, X. Enhanced machining of steel using femtosecond pulse pairs. *Appl. Phys. A* **2010**, *101*, 487–490. [CrossRef]
22. Anisimov, S.I.; Kapeliovich, B.L.; Perel'man, T.L. Electron emission from metal surfaces exposed to ultrashort laser pulses. *J. Exp. Theor. Phys.* **1974**, *39*, 375–377.
23. Chen, J.K.; Beraun, J.E. Numerical study of ultrashort laser pulse interactions with metal films. *Numer. Heat Transf. Part A* **2001**, *40*, 1–20.
24. Ren, Y.; Chen, J.K.; Zhang, Y. Optical properties and thermal response of copper films induced by ultrashort-pulsed lasers. *J. Appl. Phys.* **2011**, *110*, 113102. [CrossRef]
25. Lin, Z.; Zhigilei, L.V.; Celli, V. Electron-phonon coupling and electron heat capacity of metals under conditions of strong electron-phonon nonequilibrium. *Phys. Rev. B* **2008**, *77*, 075133. [CrossRef]
26. Courant, R.; Friedrichs, K.O. *Supersonic Flow and Shock Waves*; Interscience Publishers: New York, NY, USA, 1976.
27. Ionin, A.A.; Kudryashov, S.I.; Makarov, S.V.; Seleznev, L.V.; Sinitsyn, D.V. Generation and detection of superstrong shock waves during ablation of an aluminum surface by intense femtosecond laser pulses. *JETP Lett.* **2011**, *94*, 34–38. [CrossRef]
28. Ren, Y.; Cheng, C.W.; Chen, J.K.; Zhang, Y.; Tzou, D.Y. Thermal ablation of metal films by femtosecond laser bursts. *Int. J. Therm. Sci.* **2013**, *70*, 32–40. [CrossRef]
29. Kelly, R.; Miotello, A. Comments on explosive mechanisms of laser sputtering. *Appl. Surf. Sci.* **1996**, *96–98*, 205–215. [CrossRef]
30. Hess, H. Critical data and vapor pressures of aluminium and copper. *Z. Metallkunde* **1998**, *89*, 388–393.
31. Huang, J.; Zhang, Y.; Chen, J.K. Superheating in liquid and solid phases during femtosecond-laser pulse interaction with thin metal film. *Appl. Phys. A* **2011**, *103*, 113–121. [CrossRef]
32. Sandhu, A.S.; Dharmadhikari, A.K.; Kumar, G.R. Time resolved evolution of structural, electrical, and thermal properties of copper irradiated by an intense ultrashort laser pulse. *J. Appl. Phys.* **2005**, *97*, 023526. [CrossRef]
33. Roberts, D.E.; Plessis, A.d.; Botha, L.R. Femtosecond laser ablation of silver foil with single and double pulses. *Appl. Surf. Sci.* **2010**, *256*, 1784–1792. [CrossRef]